


L. TARTARA   
I. CRISTIANI  
V. DEGIORGIO

# Blue light and infrared continuum generation by soliton fission in a microstructured fiber

INFN and Dipartimento di Elettronica, Università degli Studi di Pavia, Via Ferrata 1, 27100 Pavia, Italy

Received: 4 February 2003

Published online: 6 June 2003 • © Springer-Verlag 2003

**ABSTRACT** The nonlinear propagation of ultrashort pulses in a microstructured fiber is experimentally investigated. By working around 800 nm, in the anomalous dispersion region, clear evidence of pulse break-up and soliton propagation is obtained. This is consistent with the recently suggested mechanism of spectral broadening based upon the fission of higher order solitons into red-shifted fundamental solitons and blue-shifted dispersive waves. When 190-fs pulses at high input intensities are used, the output spectrum is made of a broad infrared supercontinuum coexisting with a sharp and very intense blue peak that takes up to 24% of the input power. We tentatively propose an explanation of this effect by invoking pulse-trapping phenomena controlled by the group-velocity matching of infrared and visible pulses.

PACS 42.65.Tg; 42.81.Dp

## 1 Introduction

In recent years the development of microstructured fibers (MFs) [1] has made possible the observation of amazing nonlinear phenomena exploiting the silica third-order susceptibility. The nonlinear efficiency of MFs is highly enhanced with respect to standard optical fibers because the fundamental propagation mode can be confined to a very small area. Moreover the anomalous dispersion region can be shifted towards much lower wavelengths than those attainable with standard fibers, allowing soliton propagation into the visible range.

Several experiments performed with ultrashort laser pulses in MFs report the generation of a broadband supercontinuum [2–8] and sharp spectral lines coming from harmonic generation and four-wave-mixing effects [8–11]. Great attention has been recently devoted to the investigation of the dynamics of supercontinuum generation in the anomalous dispersion region near the zero dispersion wavelength  $\lambda_{ZD}$ . It has been demonstrated that the generation and the evolution of supercontinuum radiation in that region is governed by the fission of high order solitons [12, 13]. As a consequence, the

output spectrum consists of a broad-band infrared component due to the red-shifted fundamental solitons and a blue-shifted dispersive wave.

We describe here the results of a detailed experimental investigation of the nonlinear propagation of ultrashort pulses near  $\lambda_{ZD}$  in a MF, performed by varying the input power, input wavelength, and pulse duration. By using femtosecond pulses, we present clear evidence of pulse break-up and solitonic propagation. At small and moderate input intensities our results follow the trends described in [12] and [13]. At high input intensities, we find that the visible part of the output spectrum is made of a sharp and very intense peak in the blue region. The blue light propagates in the fundamental mode and can collect up to one fourth of the input power. We suggest that such a striking result, not predicted by the simulations of [12], could be connected to a pulse-trapping effect triggered by the group-velocity matching between the soliton and the dispersive wave. We also present results obtained by using picosecond pulses. The soliton dynamics leading to the generation of the infrared supercontinuum and visible radiation is still observable, but with different characteristics when compared to the femtosecond-pulse case.

## 2 Experiment

The MF under investigation was fabricated at the Optoelectronics Research Center (Southampton, U.K.). It is characterized by a very small core diameter (about 1.5  $\mu\text{m}$ ) that enhances its nonlinear properties and by an asymmetry in the core region that induces a high birefringence leading to a polarization maintaining behavior [5, 8]. A scanning electron microscope picture of the fiber is presented in Fig. 1 of [8].

First of all we checked the dispersion properties of the fiber. We simulated the modal behavior of our MF by using a software program (BPM *RSOFT*) based on the beam-propagation method. As the input profile for the simulation the real fiber section was used. While the dispersion behavior obtained by the simulation is quite reliable, the estimated value of the zero dispersion wavelength  $\lambda_{ZD}$  has a limited accuracy, because of the intrinsic precision of the propagation software. In order to compare the simulation with experiment it should also be taken into account that the fiber cross-section might have some structural variation along the span, so that

✉ Fax: +39-0382/422-583, E-mail: tartara@ele.unipv.it

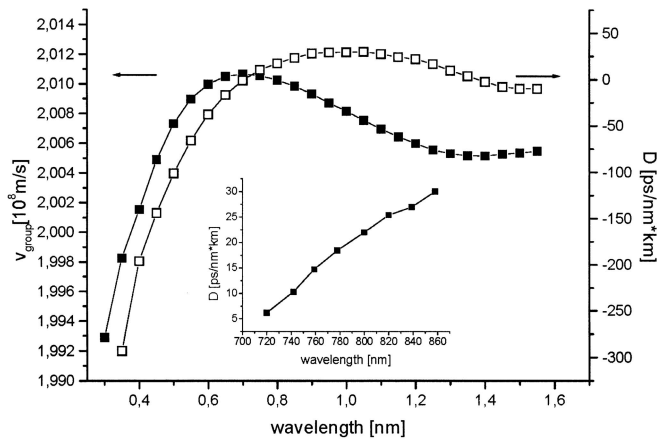


**FIGURE 1** Simulated group velocity  $v_g$  and group-velocity dispersion  $D$  of the microstructured fiber plotted as functions of wavelength. The inset shows experimental data concerning  $D$  vs.  $\lambda$  over a limited  $\lambda$ -range

during propagation, the pulse experiences the effect of an average dispersion. To calibrate the simulation results we experimentally measured the group velocity dispersion on a 2-m-long fiber span in the wavelength range 700–860 nm by using a technique similar to that described in [14]. The results are reported in the inset of Fig. 1. By extrapolating the data, we obtained that  $\lambda_{ZD}$  is close to 700 nm. The simulated fiber group-velocity and group-velocity-dispersion  $D$  [15] are reported as functions of wavelength in Fig. 1. The fiber presents a second zero-dispersion wavelength around 1500 nm.

To investigate the MF nonlinear behavior around  $\lambda_{ZD}$ , we used a Titanium Sapphire laser (Tsunami Spectra Physics) tunable in the wavelength range 700–900 nm. The laser emits a 110-fs transform-limited pulse train at an 80 MHz repetition rate. In order to avoid back-reflections from the input end of the fiber into the laser source we had to use a Faraday isolator that broadened the pulse-width up to 190 fs. The input beam was linearly polarized along one of the principal polarization axes of the MF. The length of the MF was 40 cm. The results described here all refer to situations in which the input radiation was coupled to the fiber fundamental mode, and in which the observed output radiation, both infrared and visible, was also in the fundamental mode. In the experiment we measured the total optical power at the fiber output. This was only slightly smaller than the power coupled inside the fiber, taking into account that the linear attenuation coefficient of our fiber was about  $0.3 \text{ m}^{-1}$  in the investigated range of wavelengths. The maximum power measured at the fiber output was about 100 mW.

We measured the output optical spectra obtained by tuning the Titanium Sapphire laser at  $\lambda_{IN} = 810 \text{ nm}$ , and increasing progressively the average input power  $P_{IN}$ . Some typical spectra are shown in Fig. 2. We found in each spectrum two well-separated components, a red-shifted wide one and a blue-shifted narrow one, both consisting of a sequence of peaks. We observed that, as  $P_{IN}$  was increased, the average central wavelength of the infrared radiation became larger and that of the visible line became smaller, as shown by the spectra presented in Fig. 2. In particular the visible line wavelength shifted from 530 to 430 nm as  $P_{IN}$  was increased from 10 to 50 mW. The number of infrared peaks can be related to the

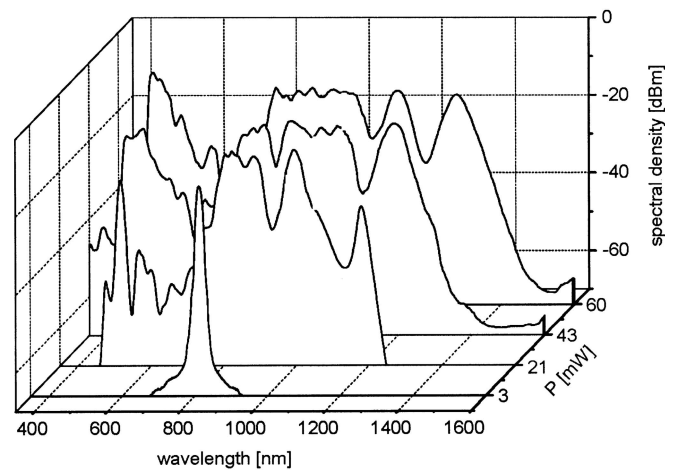


**FIGURE 2** A set of output spectra obtained with 190-fs 810-nm pulses for increasing average input power

soliton number  $N$ , defined by  $N^2 = \gamma P_0 L_D$ , where  $\gamma$  is the fiber nonlinear coefficient,  $P_0$  is the peak power, and  $L_D$  is the dispersion length [15]. In the investigated range of input powers  $N$  varied from 1 to 5. Each peak in the spectrum should correspond to an ultrashort pulse in the time domain.

By considering in particular the spectrum obtained at  $P_{IN} = 35 \text{ mW}$ , shown in Fig. 3a with a linear scale to make the structure more evident, we obtained evidence of pulse splitting through an intensity autocorrelation experiment performed relative to the peak at 1100 nm (marked by an arrow). The result, shown in Fig. 3b, represents very clear evidence of soliton fission in the time domain. The full width at half height of the correlation function was 85 fs, corresponding to a pulse duration  $\tau_p$  of 55 fs, much shorter than that of the input pulse. The full width at half height of the frequency peak  $\Delta\nu_p$  was 6.45 THz, yielding a product  $\tau_p \Delta\nu_p = 0.35$ , very close to the expected value for a transform-limited hyperbolic-secant pulse. Such a finding makes very plausible the hypothesis that the pulse was a soliton.

When the input power was increased above 50 mW, the overlap among the infrared peaks became very strong, so that an infrared supercontinuum roughly extending from 800 to 1500 nm was observed, as is shown in Fig. 4. A very different and surprising behavior was found for the visible part of the spectrum: instead of merging different peaks into a broad visible supercontinuum, the nonlinear propagation concentrated the visible intensity into a huge peak at 430 nm with a width of a few nanometers. As shown by the spectrum in Fig. 4 the visible peak could be more than 10 dB above the level of the generated infrared supercontinuum. At  $P_{IN} = 75 \text{ mW}$  the power  $P_{VIS}$  associated with the blue line at 430 nm was 18 mW, giving a conversion efficiency  $\eta = P_{VIS}/P_{IN} = 24\%$ . It is important to note that the blue light propagates as a fundamental mode of the MF.

We verified experimentally and by the numerical simulations that the fiber was multimodal at 810 nm. As a consequence, the conversion efficiency was critically dependent on the coupling conditions, so that considerable generation of blue light was obtained only when the input beam was mainly coupled to the fiber fundamental mode. Although other previous experiments have shown generation of blue light, such

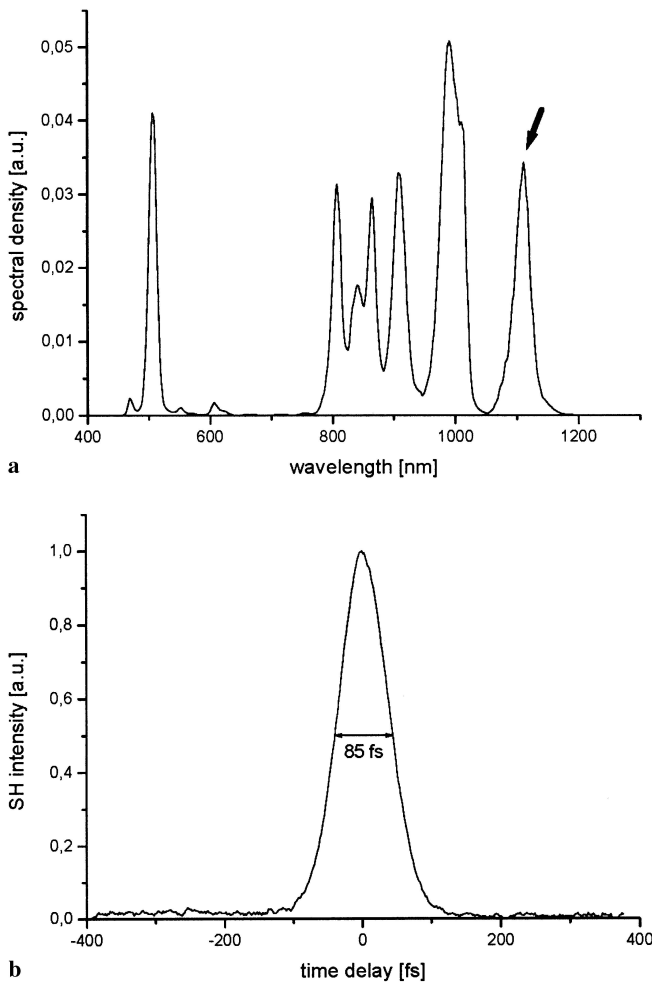


**FIGURE 3** **a** Output optical spectrum, on a linear scale, at 810 nm observed at an average input power of 35 mW. **b** Intensity autocorrelation function relative to the peak marked with an arrow in **a**

a large efficiency in the generation of narrow-band blue light has never been reported in the literature, and it has been not predicted by the available simulations.

The observed behavior was very stable and reproducible and did not depend critically on the fiber length. In fact we repeated the experiment with a 20-cm-long span of MF and found the same multi-peak structure: in this latter case each peak was even sharper and better defined.

Subsequently we checked the supercontinuum behavior by varying the input wavelength. We verified that the separation between the two components increased as the input wavelength was increased far away from  $\lambda_{ZD}$  (Fig. 5). On the contrary, when the wavelength approached  $\lambda_{ZD}$  we observed that the supercontinuum had a narrower extension and the separation between blue and infrared radiation disappeared completely.

As foreseen by the higher order soliton fission theory, the number of infrared peaks decreased as the wavelength was pushed away from the  $\lambda_{ZD}$ : in fact the group velocity dispersion became larger, leading to a decrease of the soliton number.

The numerical simulations and the experimental work about soliton fission in MFs have been carried out until now

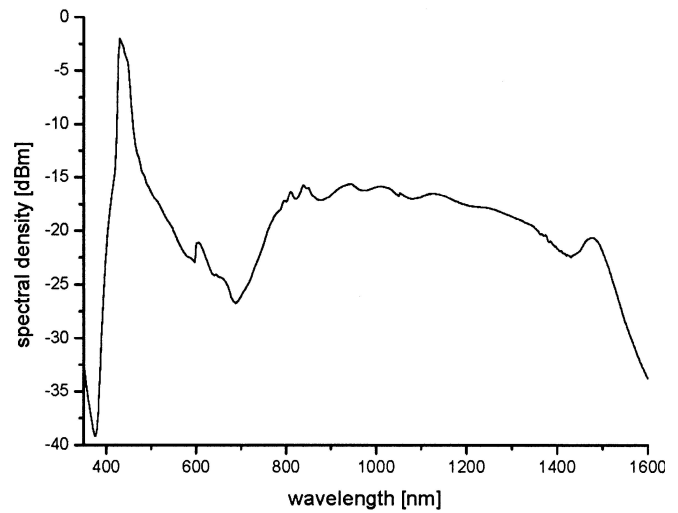


**FIGURE 4** Output optical spectrum, on a log-scale, at 810 nm observed at an average input power of 75 mW

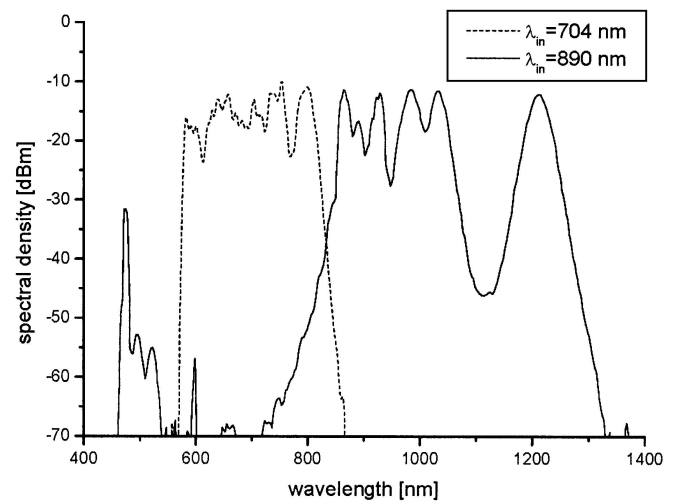


**FIGURE 5** Comparison between the output optical spectra obtained at 704 and 890 nm for similar input powers

with pulses having durations no longer than 200 fs. We decided to use picosecond pulses in order to verify whether the same soliton dynamics is still effective when the pulse duration is increased. We configured the laser cavity in order to emit a 1.3 ps transform-limited pulse train. In this situation the maximum attainable peak power was about 1 kW. We used a 95-cm-long fiber as we noticed a slower dynamics of the phenomena.

The behavior we found in our measurements was qualitatively similar to that with femtosecond pulses, the main differences being from a quantitative point-of-view. In Fig. 6 we report the evolution of the supercontinuum obtained by tuning the laser wavelength at 810 nm. For the same average power and wavelength used for the femtosecond pulses, the soliton number was increased by the longer pulse-width. Furthermore, four-wave mixing processes were favored because of a larger temporal overlap between the pulses arising from the fission process. Both these aspects lead very likely to a good flatness of the supercontinuum, regardless of the input wavelength. The spectral broadening was reduced compared with the femtosecond case, as the main mechanism of

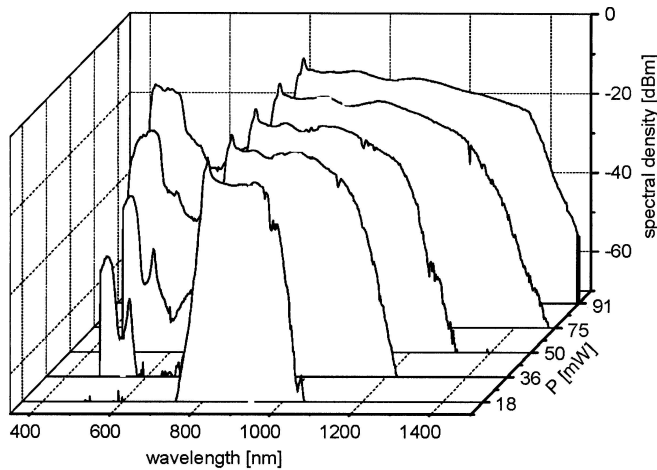


**FIGURE 6** A set of output spectra obtained with 1-ps 810-nm pulses for increasing average input power

the supercontinuum evolution after the initial fission is soliton self-frequency shift whose magnitude is proportional to the inverse of the fourth power of the pulse-width [16].

We notice that the visible radiation generation was less effective when using picosecond pulses. The strongest visible peak was at best at the same level as the infrared continuum and it disappeared from the output spectrum as the input wavelength was increased above 860 nm.

### 3 Discussion

Several papers have reported experimental evidence of supercontinuum generation by fission of higher order solitons propagating close to  $\lambda_{ZD}$  in MFs. In all the reported data the supercontinuum coexists with an anti-Stokes blue radiation. The physical origin of such radiation is not completely understood. [12] gives evidence that soliton dynamics plays a crucial role in the propagation of ultrashort pulses in the anomalous dispersion region of the MF and presents an explanation for visible light generation based on a phase relation between solitons and dispersive waves.

Following the approach proposed in [12], we relate the multi-peak structure of the infrared supercontinuum to the evolution and fission of higher order solitons. The third-order dispersion induces the progressive decay of the  $N$ -soliton into its  $N$  constitutive fundamental solitons [15, 17]. The input pulse breaks up into a fundamental soliton and a  $(N-1)$ -soliton, which undergoes the same dynamics, turning into a  $(N-2)$ -soliton and so on [18]. It is well known that a soliton propagating in a perturbed regime experiences a dynamical evolution of its parameters. This process is accompanied by a loss of energy that is progressively transferred to dispersive radiation. The simple phase-matching condition proposed in [12] is not adequate, in our opinion, to describe the generation of the visible part of the spectrum. In fact the spectral components of the dispersive radiation must belong initially to the soliton optical spectrum [19]. Any subsequent frequency shift must be explained by invoking some nonlinear interaction to guarantee the fundamental energy conservation principle. The radiation is emitted around the point of strong temporal compression of the higher order soliton [18],

when the short-wavelength tail of the spectrum has deeply extended even into the normal dispersion region. The intensity of the dispersive radiation in the normal dispersion regime can also be coherently enhanced by the presence of a resonance frequency in the soliton tail. The resonance condition is determined by the effect of third-order dispersion [19]. The resonant peak in the normal dispersion regime can be easily observed in Fig. 7, in which the output spectrum at a power of 11 mW and a wavelength of 738 nm is reported. The subsequent evolution of the fundamental solitons is driven by the self-frequency shift induced by intra-pulse stimulated Raman scattering [20–22]. The pulse is shifted toward longer wavelengths. As we observed experimentally the dispersive radiation emitted on the blue-shifted side of the soliton spectrum behaves like an anti-Stokes wave that progressively shifts towards the visible spectral region [20–22]. Many different interpretations have been reported [12, 20] to describe this peculiar behavior. However, the observed growth of the huge blue peak at a fixed wavelength cannot easily be explained in the framework of those interpretations.

We believe that the evolution of anti-Stokes radiation can be satisfactorily explained by the mechanism of pulse trapping across the zero-dispersion wavelength, which has been recently demonstrated [23]. In this phenomenon an optical pulse in the normal dispersion region is trapped by a soliton pulse in the anomalous dispersion region and then the two pulses copropagate along the fiber. The anti-Stokes radiation experiences a cross-phase modulation due to the solitons that propagate in the anomalous dispersion regime and progressively shift towards longer wavelengths. As shown in Fig. 1 the soliton group velocity continuously decreases during the Raman shifting process; the cross-phase modulation traps the anti-Stokes radiation, leading to a blue-shift up to a wavelength that makes the group velocities of the two waves equal.

In our specific case the dependence of the group velocity on wavelength is rather weak in the range 1.1–1.6  $\mu\text{m}$ , so that many different solitons are group-matched with the dispersive radiation in a narrow spectral region lying around 450 nm. This fact could explain the growth of the huge peak, as many solitons trap the dispersive radiation around the same

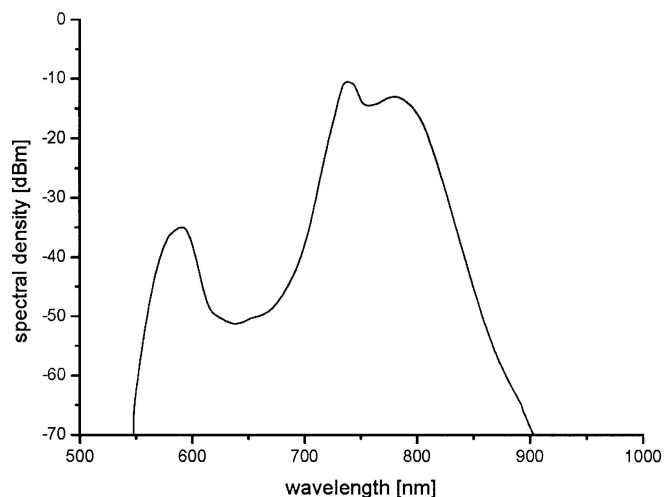


**FIGURE 7** Output optical spectrum with 1.3-ps 738-nm input pulses at an average input power of 11 mW

wavelength. In addition, the trapping effect combined with the dispersive behavior of the fiber should lead also to the saturation of the shifting wavelength that we experimentally observed. In fact, as shown in Fig. 2, by increasing the input power we see initially a progressive wavelength shift of the dispersive radiation up to about 430 nm. Above this point, by increasing the power we observe that the anti-Stokes intensity progressively increases, while its central wavelength experiences a negligible shift.

#### 4 Conclusions

Our experimental investigation of the nonlinear propagation of femtosecond pulses near the zero-dispersion wavelength of a microstructured fiber shows clear and direct evidence of pulse break-up and soliton propagation. At moderate input intensities the output spectrum consists of two well-separated components, one in the infrared and the other in the visible, each appearing as a sequence of peaks. At high input intensities the spectrum is made of a broad infrared supercontinuum coexisting with a rather sharp peak in the visible. Our results are consistent with the scenario proposed in [12]. A striking feature of our data, not appearing in previous experiments and simulations, is that the generated visible wave has a very large intensity and little broadening. We tentatively propose an explanation of this effect based on the pulse-trapping phenomena associated with the group-velocity matching of infrared and visible pulses. In principle it should be possible to optimize the efficiency of conversion from infrared to blue radiation (maybe even going beyond the obtained 24%) by an appropriate design of the microstructured fiber, together with a clever choice of the input wavelength.

**ACKNOWLEDGEMENTS** We thank D.J. Richardson and coworkers for the fabrication of the microstructured fiber, and M. Romagnoli and coworkers for the simulation results.

#### REFERENCES

- 1 J.C. Knight, J. Broeng, T.A. Birks, P.S.J. Russell: *Science* **282**, 1476 (1998)
- 2 J.K. Ranka, R.S. Windeler, A.J. Stentz: *Opt. Lett.* **25**, 25 (2000)
- 3 S. Coen, A.H.L. Chau, R. Leonhardt, J.D. Harvey, J.C. Knight, W.J. Wadsworth, P.S.J. Russell: *Opt. Lett.* **26**, 1356 (2001)
- 4 S. Coen, A.H.L. Chau, R. Leonhardt, J.D. Harvey, J.C. Knight, W.J. Wadsworth, P.S.J. Russell: *J. Opt. Soc. Am. B* **19**, 753 (2002)
- 5 J.H.V. Price, W. Belardi, T.M. Monro, A. Malinowski, A. Piper, D.J. Richardson: *Opt. Express* **10**, 382 (2002)
- 6 J.M. Dudley, L. Provino, N. Grossard, H. Maillotte, R.S. Windeler, B.J. Eggleton, S. Coen: *J. Opt. Soc. Am. B* **19**, 765 (2002)
- 7 A.B. Fedotov, A.N. Naumov, A.M. Zheltikov, I. Bugar, D. Chorvat, Jr., D. Chorvat, A.P. Tarasevitch, D. von der Linde: *J. Opt. Soc. Am. B* **19**, 2156 (2002)
- 8 L. Tartara, I. Cristiani, V. Degiorgio, F. Carbone, D. Faccio, M. Romagnoli, W. Belardi: *Opt. Commun.* **215**, 191 (2003)
- 9 A.N. Naumov, A.B. Fedotov, A.M. Zheltikov, V.V. Yakovlev, L.A. Melnikov, V.I. Beloglazov, N.B. Skibina, A.V. Shcherbakov: *J. Opt. Soc. Am. B* **19**, 2183 (2002)
- 10 J.K. Ranka, R.S. Windeler, A.J. Stentz: *Opt. Lett.* **25**, 796 (2000)
- 11 F.G. Omenetto, A.J. Taylor, M.D. Moores, J. Arriaga, J.C. Knight, W.J. Wadsworth, P.S.J. Russell: *Opt. Lett.* **26**, 1158 (2001)
- 12 A.V. Husakou, J. Herrmann: *Phys. Rev. Lett.* **87**, 203901 (2001)
- 13 J. Herrmann, U. Griebner, N. Zhavoronkov, A. Husakou, D. Nickel, J.C. Knight, W.J. Wadsworth, P.S.J. Russell, G. Korn: *Phys. Rev. Lett.* **88**, 173901 (2002)
- 14 D. Ouzounov, D. Homoelle, W. Zipfel, W.W. Webb, A.L. Gaeta, J.A. West, J.C. Fajardo, K.W. Koch: *Opt. Commun.* **205**, 219 (2002)
- 15 G.P. Agrawal: *Nonlinear Fiber Optics* (Academic Press, San Diego 1995)
- 16 J.P. Gordon: *Opt. Lett.* **11**, 662 (1986)
- 17 Y. Kodama, A. Hasegawa: *IEEE J. Quantum Electron.* **QE-23**, 510 (1987)
- 18 P.K.A. Wai, C.R. Menyuk, Y.C. Lee, H.H. Chen: *Opt. Lett.* **11**, 464 (1986)
- 19 N. Akhmediev, M. Karlsson: *Phys. Rev. A* **51**, 2602 (1995)
- 20 B. Washburn, S. Ralph, R. Windeler: *Opt. Express* **10**, 575 (2002)
- 21 J.M. Dudley, X. Gu, L. Xu, M. Zimmel, E. Zeek, P. O'Shea, R. Trebino, S. Coen, R. Windeler: *Opt. Express* **10**, 1215 (2002)
- 22 G. Genty, M. Lehtonen, H. Ludvigsen, J. Broeng, M. Kaivola: *Opt. Express* **10**, 1083 (2002)
- 23 N. Nishizawa, T. Goto: *Opt. Express* **10**, 1151 (2002)